ABCM Symposium Series in Mechatronics - Vol. 1 - pp.682-687
Copyright © 2004 by ABCM

Microgrippers Driven by Electrostatic Comb Drive Actuators

Vitório Arrivabeni Longo de Almeida
University of Sao Paulo, Polytechnic School, Department of Mechatronic and Mechanical Systems Engineering
Av. Prof. Mello Moraes, 2231 / CEP: 05508-030 / Sao Paulo - SP / Brazil

Paulo Henrique de Godoy
University of Sao Paulo, Polytechnic School, Department of Mechatronic and Mechanical Systems Engineering
Av. Prof. Mello Moraes, 2231 / CEP: 05508-030 / Sao Paulo - SP / Brazil

Emilio Carlos Nelli Silva
University of Sao Paulo, Polytechnic School, Department of Mechatronic and Mechanical Systems Engineering
Av. Prof. Mello Moraes, 2231 / CEP: 05508-030 / Sao Paulo - SP / Brazil
ecnsilva@usp.br

Ricardo Cury Ibrahim
University of Sao Paulo, Polytechnic School, Department of Mechatronic and Mechanical Systems Engineering
Av. Prof. Mello Moraes, 2231 / CEP: 05508-030 / Sao Paulo - SP / Brazil
ricardo.ibrahim@poli.usp.br

Abstract. In this work we report the design and fabrication of linear electrostatic comb-drive actuated microgrippers. The actuators have been fabricated by surface micromachining of electroplated copper and nickel films. The fabrication is simple and includes UV lithography, electrodeposition, and wet etching processes. The fabrication characteristics are also discussed. The comb-drive structures feature fingers with different widths and gaps, and flexible hinges with a unidirectional linear actuation scheme. The comb-drive behavior is theoretically described with equations. The actuators have been simulated by finite element electromechanical models, which revealed important data such as motion behavior, operation conditions and stress concentration regions. The motion dependence on drive voltage for both cases were measured and compared with predictions from the simulation models. The models also included different schemes for the hinges supporting the driving section of the comb drive and the presented simulation results showed the effects of these "springs" on motion behavior.

1. Introduction

Microelectromechanical systems (MEMS) are attracting much attention from researches of various fields due to their wide range of applications. Research on MEMS gathers several disciplines with a common objective of developing tools for studying the so called "microworld". Various branches of science are interested on improving the comprehension of microscopic systems, giving birth to the microscience. This improvement requires the development of new instruments (microactuators and microsensors) which is done using new design methods.

Microactuators find applications in precision equipments such as micropositioning systems, microvalves, micropumps, and micromanipulation devices such as microgrippers (Volland, 2002). The technological advancements towards the investigation of the microworld make it necessary to develop new tools capable of interacting with the ambient around them. In microelectronics, for example, modern equipment for lithography requires high precision positioners with submicrometric resolutions as the MOS technology advances towards faster devices. Further, the road to nanotechnology has led to new equipments such as the atomic force microscope (ATM) and the scanning tunneling microscope (STM). The expansion of microbiology led to the creation of new micromanipulation equipments such as microgrippers, microvalves and micropumps. The miniaturization of typical macroscopic mechanisms is possible only with alternative actuation methods to overcome the limitations of conventional methods. One example is the electromagnetic actuation, widely used in automatic systems trough stepped motors. In microscopic dimensions, this method shows expressive loss of efficiency compared to other methods such as electrostatic, piezoelectric and electrothermal actuators.

Electrostatic actuation is one of the simplest actuation methods. Inside this group of actuators the most widely used are the comb-drives (Johnson, 1995).

Comb-drives can be used either for electrostatic actuation or capacitive sensors (Yeh *et al*, 2000). Comb drives are made of two combs, a movable one and a fixed one, where an electrical potential difference between them generates an attraction force, moving the movable comb. The family of comb-drives can be classified into interdigitated comb-drives and asymmetric comb-drives. Using interdigitated comb-drives motion occurs parallel to the fingers (one comb cases the other) while in asymmetric comb-drives motion occurs orthogonal to the fingers. In general, interdigitated comb-drives are utilized in in-plane motions. They are intended for applications in mechanical sensors, RF communication, microbiology, mechanical power transmission, long-range actuation, microphotonics, and microfluids. On the other hand, the asymmetric comb-drives are developed specifically for generating great non-planar or torsional motions. Sensors made of comb-drives, such as micromechanical filters, are capable of having their frequency response controlled by a DC polarization. Also, the asymmetric comb-drives can be used to actuate devices such as scanners and optical switches.

This paper deals with the development of a microgripper actuated by interdigitated and asymmetric comb-drives. These microgrippers were fabricated in copper and nickel by two different fabrication processes, which have their

characteristics also presented.

The microgrippers were designed according to the available fabrication processes characteristics and their behavior was characterized through experimental measurements and computational simulations.

2. Working Principle

Figure 1 shows a model of interdigitated comb-drive.

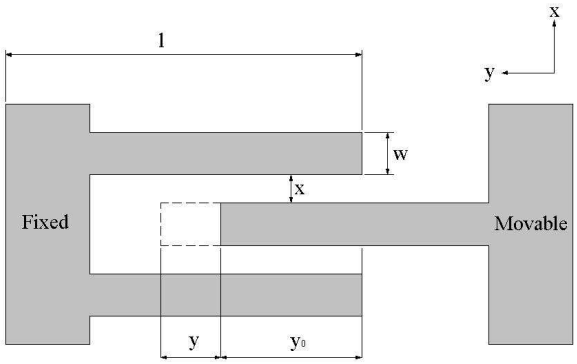

Figure 1. Model of an interdigitated comb-drive.

For the interdigitated comb-drive, the electrostatic attraction force in the y-direction exerted by the movable comb in the fixed one is given by Eq. (1).

$$F_e = \frac{dW}{dy} \tag{1}$$

Here W is the stored capacitive energy given by Eq. (2).

$$W = \frac{C_i \cdot V^2}{2} \tag{2}$$

C_i is the total capacitance of the comb, and V is the applied voltage. The total capacitance is given by Eq. (3).

$$C_i = n \cdot \varepsilon \cdot z \cdot \left[\frac{(y_0 - y)}{x} + \frac{w}{(l - y_0 - y)} \right] \tag{3}$$

Here, n is the number of fingers, ε is the permittivity between the fingers, z is the finger thickness, y_0 is the zero-voltage overlap length of the comb fingers, y is the displacement of the movable comb, x is the gap between the fingers, w is the width of the fingers, and l is the length of the fingers.

By replacing Eq. (2) and (3) in Eq. (1) we have that the electrostatic force is given by:

$$F_e = n \cdot \varepsilon \cdot z \cdot V^2 \cdot \left[\frac{1}{x} + \frac{w}{(l - y_0 - y)} \right] \tag{4}$$

For small displacements in the y-direction, the mechanical restoring force of the beam suspension is given by Eq. (5).

$$F_s = -k \cdot y \tag{5}$$

According to Horenstein *et al* (2001) the stiffness factor k is given by Eq. (6)

$$k = m \cdot \frac{3 \cdot E \cdot z \cdot w_b^{\,3}}{12 \cdot l_b^{\,3}} \tag{6}$$

where, m is the number of individual beam lengths, E is the Young modulus of the beam material, w_b is the width of the beam, and l_b is the length of the beams.

For static actuation, the electrostatic force equals the suspension beams restoring force. As a result, the voltage needed to given the movable comb a known displacement is given by Eq. (7).

$$V = \sqrt{\frac{k \cdot y}{n \cdot \varepsilon \cdot z \cdot \left[\frac{1}{x} + \frac{w}{(l - y_0 - y)}\right]}} \tag{7}$$

In the case of an asymmetric comb-drive the equations must be modified. As the movable finger is not centered between the fixed fingers there are two different capacitances C_1 e C_2 for each finger, respectively, the major gap and the minor gap capacitances. The comb capacitance C_L is the sum of the capacitances.

$$C_L = C_1 + C_2 = n \cdot \varepsilon \cdot y_0 \cdot z \cdot \left(\frac{1}{x_0 - x_d - x} + \frac{1}{x_0 + x_d + x}\right) \tag{8}$$

Here, x_0 is the symmetric gap between the fingers, x_d is the difference between the initial position of the finger and the symmetric gap, and x is the displacement of the movable comb in the x-direction.

The electrostatic force exerted by this actuator is given by Eq. (9).

$$F_{el} = F_{el,1} - F_{el,2} = \frac{\partial}{\partial x}\left(\frac{1}{2} C_1 V^2\right) - \frac{\partial}{\partial x}\left(\frac{1}{2} C_2 V^2\right) \tag{9}$$

3. Fabrication

The devices were fabricated using suspended structures of nickel. The fabrication process consisted of electroplating a copper sacrificial layer, electroplating a structural layer of nickel, and removing the copper sacrificial layer, resulting in suspended structures (surface micromachining). The electroplating of copper was realized in a bath of copper sulfate agitated at ambient temperature. The electroplating of nickel was realized in a bath of nickel chloride agitated and heated at 50°C. The masks used in this work were photolithes (a plastic film with a light sensitive resin). That type of mask restricts the attainable resolution to about 30 μm. The details are described below.

The nickel structures were fabricated by electroplating copper and nickel onto silicon or alumina substrates. The silicon wafers were (111) oriented. Both wafers had an initial 200 Å titanium layer deposited over their surface to promote the adherence between the substrate and the metallic layer required for electroplating. A 2000 Å gold layer was deposited over the titanium film generating the seed for electroplating. These two metallic films were sputtered.

The first step was to pattern the sacrificial layer. The lithographic transference of the mask pattern onto the substrate was made trough the exposure of a photosensitive polymer (photoresist) to Ultra-Violet light (UV). The photoresist was developed exposing some areas of the substrate and protecting others. The pattern was generated by a commercial CAD software and fabricated by laser printing in photolithes. The minimum dimension of the electroplated devices was 30 μm. This dimension was imposed by the fabrication process of the lithographic mask (photolith), but the electroplating process allows us to achieve sub micrometric dimension devices. The lithography was realized exposing a 20 μm thick AZ-4620 resist (Clariant) to UV light.

The next step was the electroplating of a 6 μm copper sacrificial layer. The process was realized in a bath with $CuSO_4$ and H_2O. After the growth of copper film, the second lithographic procedure took place for the transference of the nickel pattern. The electroplating of nickel was done in a heated bath of nickel chloride and water. Nickel was grown to a thickness of about 10 μm.

The bathes were prepared in beakers with magnetic agitators. The nickel bath was heated in a hot plate. The electrodes were cleaned in H_2SO_4 (10%). The samples were also cleaned in this solution just before being placed in the bathes.

The copper sacrificial layer was removed selectively in relation to the nickel layer, leaving the nickel structures suspended. This removal was done with a solution containing ammonium hydroxide (NH_4OH), hydrogen peroxide (H_2O_2) and water. The gold layer was removed in a solution based on potassium cyanide (KCN), salt 645 and water. The titanium layer was removed in a buffered HF solution. Figure 2 shows one of the comb-drives fabricated by electroplating.

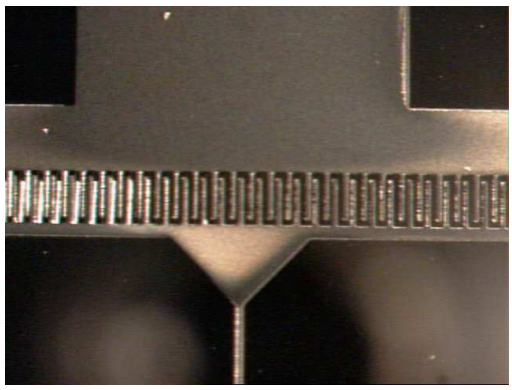

Figure 2. Photograph of an electroplated asymmetric comb-drive.

4. Results and Discussion

The majority of the nickel structures showed good results concerning the device's geometric definition, presenting roughness on the fingers' borders due to the grain size of the film. Some structures presented deformed fingers because of the large grain size. Other imperfections include structures stuck to substrates, with partial removal of the sacrificial layer due to the lack of channels for the reactant flow.

The processes showed the importance of the sample cleaning, purity of the bath solution, and current density in the electroplating processes. The purity of the solution and the current density determine the electroplated film grain size. The smaller the grain size, the better is the film quality. Some devices previously fabricated showed that large grains may damage the comb-drive's fingers. Figure 3 shows one of the comb-drives fabricated with a new solution (high purity).

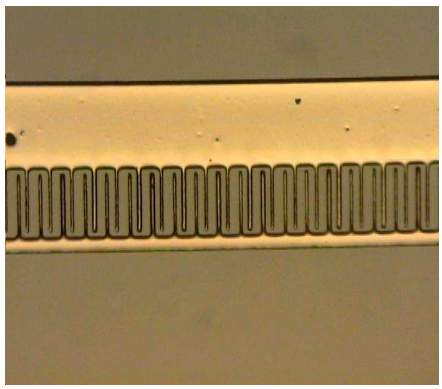

Figure 3. Photograph of the fingers of an electroplated comb-drive fabricated with a high purity solution. One can see the good geometric resolution.

The electroplated structures also showed some deformations due to residual stresses produced by the several wet processing steps (Fig. (4)). While the fixed comb structures showed no perceptible deformations, parts of movable combs had high deformations caused by residual stresses.

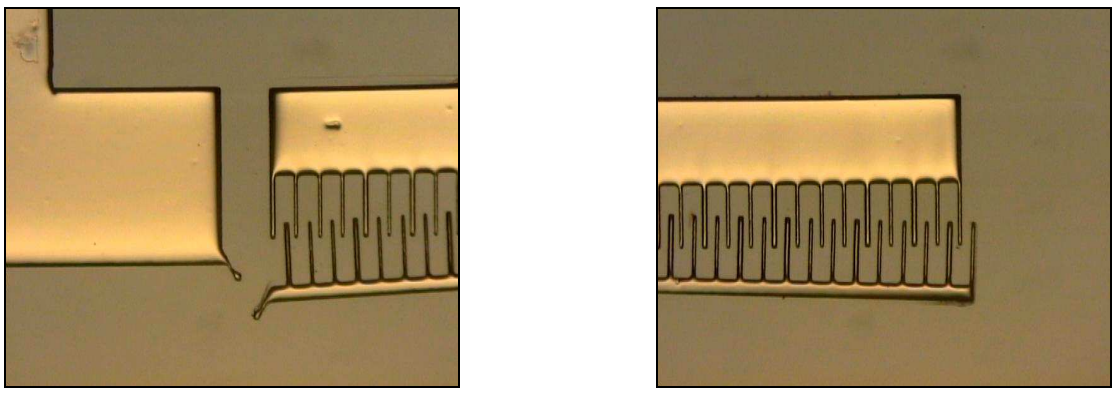

(A) (B)

Figure 4. Photographs showing the residual stress effect on parts of suspended comb-drive structures. Note that these

effects are observed only on movable combs.

The working characteristics of the nickel electroplated devices were determined applying different voltages to the pads in a probe station, and the devices were modeled by computational simulations with the software ANSYS. The displacement of the movable comb was observed in an optical microscope coupled to a CCD camera connected to a video acquisition board on a personal computer. Edition of the video frames allowed us to calculate the displacement of the movable comb structure.

Comb-drives fabricated on silicon wafers presented current leakage trough the substrate at the high voltages needed to drive them, preventing the motion of the combs.

To solve this problem, the silicon wafers were replaced by alumina substrates. Another modification adopted to improve the displacement was the development of a system for inserting the movable comb into the fixed one in order to reduce the gap between the fingers. The method is described by Hirano *et al* (1992). The basic idea is to make a comb finger with a certain width and to insert it into a gap slightly wider than the finger. This allowed us to use the same lithographic mask fabrication method but with smaller gap distances. This procedure allowed us to reduce the gaps to 5 and 10 μm.

In order to insert one comb into the other, an electrothermal actuator was coupled to the comb-drive structure, following the model proposed by Syms (1998). A voltage applied to the electrothermal actuator electrodes would bend it, because of the Joule effect induced by the current flow throughout the narrow hot arms, inserting the movable comb into the fixed one. This system introduced a different suspension set with the hot arms replacing the previous suspension beams. This system is shown in Fig. (5).

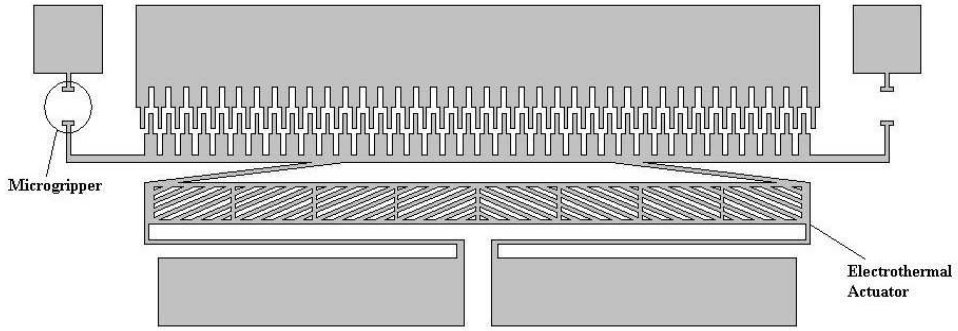

Figure 5. Design of the modified microgripper actuation system.

Figure (6) shows a photograph of the fabricated comb-drive of Fig. (5).

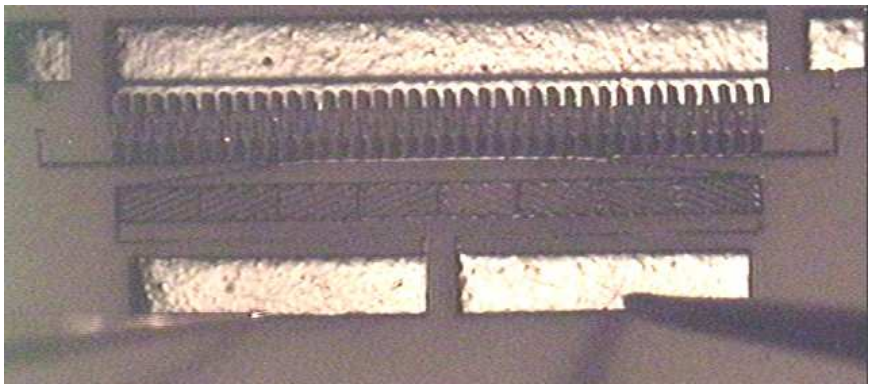

Figure 6. Photograph of the fabricated comb-drive of Fig. (5).

The finite element simulations results showed a 20 μm displament for the electrothermal actuation for a voltage of 1V, which would be sufficient to insert the movable comb into the fixed comb. The results also revealed a small warpage of the movable comb.

The devices fabricated with the system shown in Figure (5) presented high levels of residual stress in the films, causing a warpage of the suspended structure greater then the warpage showed in the simulations. This effect injured the functionality of the system. When the electrothermal actuator was activated, the movable comb mostly bended out-of-plane misaligning the comb-drive fingers.

However, when the comb-drives were actuated electrostatically only, some devices fabricated with the system of Fig (5) presented displacements of about 2 μm for high voltages (around 400 V). In many devices, the applied voltage

reached the dielectric breakdown voltage (about 500 V) before any motion could be noticed. A possible cause for this effect is the large distance between the comb-drive fingers, increasing the voltage needed to realize a given work, which can reach the air dielectric breakdown limit. A script implemented in MATLAB using the equations cited in section 2 presented similar results. Figure 7 plots the results obtained for the fabricated devices with the implemented script. The script also showed that smaller gaps greatly reduce the driving voltages.

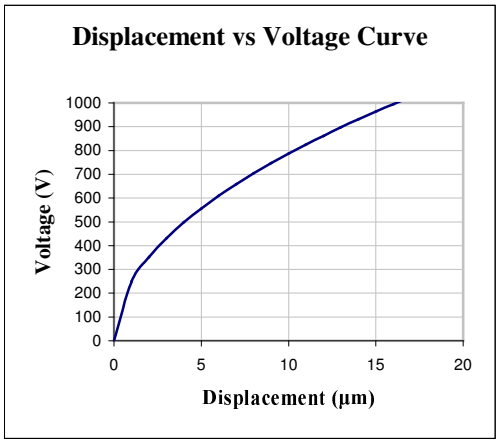

Figure 7. Theoretical response obtained with the MATLAB script.

Future works will deal with the solution of these problems. A possible solution to the warpage problem is to increase the thickness of the suspension beams, augmenting the impedance for the z-direction movement of the movable comb. Another possibility is the formation of pads under the suspended structure for electrostatic attraction of the deformed regions.

5. Conclusions

The paper presented a simple low cost MEMS fabrication method. Several comb-drives were fabricated by electroplating of nickel and wet etching of copper. The experiments showed some limitations of these micromachining processes. The results showed the importance of the sample cleaning, purity of the bath solution, and current density in the electroplating processes.

The results also showed the need for reduced dimensions. In order to improve the efficiency of the actuators the gap distances must be greatly reduced. However, the fabrication process is limited to the lithographic mask resolution. The mask used in this work had a minimum resolution of 30 µm. For smaller dimensions, the mask must be fabricated by other techniques, such as electron beam, which increases substantially the fabrication cost. With e-beam, lithographic masks can be fabricated with resolutions lower than 1 µm.

6. Acknowledgement

The authors would like to thanks the Brazilian Synchrotron Light Laboratory (LNLS) for the use of its Microfabrication Laboratory, where most of this work was done. The authors also would like to thanks Prof. Francisco Javier Ramirez Fernandes, Department of Electronics of the Polytechnic School of the University of Sao Paulo for the use of the probe station.

7. References

Hirano, T., Furuhata, T., Gabriel, K.J., and Fujita, H., 1992, “Design, Fabrication, and Operation of Submicron Gap Comb-Drive Microactuators”, J. of Microelectromechanical Systems, Vol. 1, No. 1, pp. 32-59.

Horenstein, M.N. and Stone, P.R., 2001, “A micro-aperture electrostatic field mill based on MEMS technology”, J. of Electrostatics, 51-52, pp. 515-521.

Johnson, W.A. and Warne, L.K., 1995, “Electrophysics of Micromechanical Comb Actuators”, J. of Microelectromechanical Systems, Vol. 4, No. 1, pp. 49-59.

Syms, R.R.A., 1998, “Electrothermal Frequency Tuning of Folded and Coupled Vibrating Micromechanical Resonators”, J. of Microelectromechanical Systems, Vol. 7, No. 2, pp. 164-171.

Volland, B.E., Heerlein, H. and Rangelow, I.W., 2002, “Electrostatically driven microgripper”, Microelectronic Engineering, 61–62, pp. 1015–1023.

Yeh, J.-L.A., Hui, C.-Y. and Tien, N.C., 2000, “Electrostatic Model for an Asymmetric Combdrive”, J. of Microelectromechanical Systems, VOL. 9, NO. 1,